

1-4-2024

Tepehan Rockslide: A large-scale earthquake-induced geological structure formed by Mw:7.8 Kahramanmaraş (Pazarcık) earthquake, Türkiye

ÖKMEN SÜMER
okmen.sumer@deu.edu.tr

Follow this and additional works at: <https://journals.tubitak.gov.tr/earth>



Part of the [Earth Sciences Commons](#)

Recommended Citation

SÜMER, ÖKMEN (2024) "Tepehan Rockslide: A large-scale earthquake-induced geological structure formed by Mw:7.8 Kahramanmaraş (Pazarcık) earthquake, Türkiye," *Turkish Journal of Earth Sciences*: Vol. 33: No. 1, Article 4. <https://doi.org/10.55730/1300-0985.1897>
Available at: <https://journals.tubitak.gov.tr/earth/vol33/iss1/4>

This Article is brought to you for free and open access by TÜBİTAK Academic Journals. It has been accepted for inclusion in Turkish Journal of Earth Sciences by an authorized editor of TÜBİTAK Academic Journals. For more information, please contact academic.publications@tubitak.gov.tr.

Tepehan Rockslide: A large-scale earthquake-induced geological structure formed by Mw:7.8 Kahramanmaraş (Pazarcık) earthquake, Türkiye

Ökmen SÜMER^{*}

Department of Geological Engineering, Faculty of Engineering, Dokuz Eylül University, İzmir, Türkiye

Received: 07.04.2023 • Accepted/Published Online: 01.06.2023 • Final Version: 04.01.2024

Abstract: Three devastating and powerful earthquakes hit the southeastern and eastern parts of Türkiye and the northeastern part of Syria in February of 2023, causing many earthquake-induced slope movements. One of these major mass movements is called the “Tepehan Rockslide”, which was formed by the first Mw: 7.8 earthquake on February 6th, 2023 at Pazarcık (Kahramanmaraş) located in the Altınözü district of Hatay province. The rockslide involved the movement of Middle Miocene basement rocks that consist of clayey limestone, marl, and fine-grained clastic sedimentary rocks. The morphogenetic evaluation of the structure reveals that the Tepehan Rockslide is a very rapidly developed translational interrupted ridge type earthquake-induced large-scale rockslide or a large rock glide that was formed at a distance of 19 km from the surface rupture and 136 km from the earthquake epicentre. Field observations and centimeter-precise numerical data via high resolution Unmanned Aerial Vehicle (UAV) footage with a GNSS-RTK mounted module reveal that the approximately E-W oriented longest axis of the structure is 496 m, and the widest profile is 184 m, extending in N-S direction. The total moving mass has been calculated to cover ca. 71,000 m² surface area, with an average volume of at least 1.1 million m³ and total a weight of 2.75 megatons. Comparisons made with its counterparts worldwide show that the Tepehan Rockslide is not a unique earthquake-induced slope movement by itself. However, it is the largest of the detected voluminous rockslide type slope movements formed in the region during the February 2023 earthquakes.

Key words: Devastating earthquake, earthquake-induced rockslide, Middle Miocene sedimentary sequences, surface rupture, epicentre distance, global-scale comparison

1. Introduction

Types, mechanisms, and processes of slope movements have been studied since the end of the 19th century (e.g., Baltzer, 1875). The developments in the modern scientific period on the subject have gained momentum since the 1950s (e.g., Varnes, 1978; Cruden and Varnes, 1996; Highland and Bobrowsky, 2008; Clague and Stead, 2012). Although studies especially focusing on earthquake-induced slope movements have been developed starting from the mid-1940s (e.g., Imamura, 1946; Hadley, 1960; Seed, 1968), Keefer (1984) has founded and created a starting point for constructing the earthquake-induced slope movement mechanisms. Such studies had been accelerated since the late 1990s (e.g., Rodríguez et al. 1999; Papadopoulos and Plessa, 2000; Keefer, 2002; Yamada et al., 2013; Tanyaş et al., 2017). Although these inventory-based studies are distributed from many countries and geographical regions all around the world, they mainly cluster in the USA, Japan, China, Iran, Taiwan, Indonesia, Chile, and Peru.

For Türkiye, such studies are very few such studies in the instrumental period that are associated with a known earthquake. These encompass the several large landslides (more than 500) that were triggered by the March 13th, 1992 Erzincan Earthquake (cf. Hencher and Acar, 1995; Acar, 1997), underwater and/or near-shore slope movements that occurred in the August 17th, 1999 İzmit earthquake (cf. Çetin, 2004; Kuşçu et al. 2005; Aydan et al., 2008), continental landslides formed by 1999 İzmit and Kocaeli and 2000 Orta earthquakes (cf. Duman et al., 2005), Görüm (2016) also reported more than 70 landslides for 2011 Van earthquake, and recently the landslides developed by the January 24th, 2020 Sivrice (Elazığ) earthquake (cf. Karakaş et al., 2021, Köküm, 2021). On the other hand, the only known earthquake-induced landslide, which is reported before the instrumental period and supported by absolute dating methods, is the Sünnet landslide, which is located on and connected with North Anatolian Fault Zone (Oçakoğlu et al. 2023). It is noteworthy that there is very limited scientific literature related with the earthquake-

* Correspondence: okmen.sumer@deu.edu.tr

induced slope movements in Anatolia, a terrain where there is intense and large earthquake activity throughout its existence.

In this study, a recent earthquake-induced geological structure, which occurred in the Tepehan neighborhood of the Altınözü district of Hatay province in Türkiye, is examined and evaluated for the first time via field observations and centimeter-precise GNSS-RTK readings using an Unmanned Aerial Vehicle (UAV). The field study has been conducted right after the earthquake. A comparison in terms of formation mechanism and type of this newly induced structure with the counterparts worldwide is also discussed at the final part of the paper.

2. Tectonic and geological setting of the study area

The eastern and southeastern parts of Anatolia represent an area formed by the relative movements of the Arabian, African, and Eurasian plates between each other during the Neotectonic period. This geodynamic interaction in the eastern Mediterranean creates Neotectonic structures developed in different deformation styles, at the eastern, central, and western parts of the Anatolian plate (Figure 1a) (e.g., Dewey and Şengör, 1979; Şengör et al. 1985; Barka, 1992). The region where the tectonic pattern is controlled by the compressional and strike-slip dominant stress regimes comprises a few micro-blocks basically constrained by the North Anatolian Fault Zone (NAFZ) in the north, the East Anatolian Fault Zone (EAFZ) in the west, the Dead Sea Fault Zone (DSFZ) in the south, and the Bitlis-Zagros Suture Zone (BZSZ) in the east (Figure 1b). Although the initial rigorous study focusing on the tectonic framework of the region started with Oswald (1906) who initially marked the faults on his regional maps, the EAFZ, which is related with the main subject of this study, was first illustrated roughly and piece by piece by Sieberg (1932), who evaluated the historical earthquakes and fractures together. Pınar and Lahn (1952), have shown the fault and fracture systems in their work, which was an earthquake-focused study. However, this tectonic structure was mapped for the first time by Arpat and Şaroğlu (1972), in the northeastern section between Karlıova and Hazar Lake, and named as the East Anatolian Fault. The authors also emphasized its left lateral identity in their work. Although there is a consensus in the literature about the beginning of the fault zone in Karlıova at the northeastern termination, there are different approaches to its continuity to the southeast, length, geometry, and segmentation (e.g., McKenzie, 1976; Lovelock, 1984; Muehlberger and Gordon; 1987; Perinçek and Çemen, 1990; Tatar et al., 2004; Herece, 2008; Karabacak et al., 2012; Duman and Emre, 2013; Yönlü et al. 2017; Emre et al. 2018). Although the new scientific data that emerged in the last earthquakes have revealed the necessity of

debating these scientific views in the literature, a detailed description of the EAFZ is beyond the scope of this paper, and readers are referred to Karabacak et al. (2012) and Duman and Emre (2013) for further information.

3. Kahramanmaraş (Pazarcık) earthquake parameters

Three devastating earthquakes occurred in the eastern and southeastern parts of Türkiye in February of 2023. The first big one was on February 6th at Pazarcık (Kahramanmaraş), and the second big one contiguously occurred at Elbistan (Kahramanmaraş) in the same day, nine h later. The last one took place during the field studies on February 20th at Defne (Hatay) within the impact area of the Antakya Fault Zone with a Mw: 6.4 (AFAD self-acting Focal Mechanism Solution, 2023, EMSC; European-Mediterranean Seismological Centre). The first earthquake occurred in the Türkoğlu-Pazarcık, Erkenek, and Amanos segments, which are included in the Eastern Anatolian Fault Zone, and the second one occurred on the Çardak Fault, the western termination of the Sürgü Fault and southwestern part of the Doğanşehir Fault Zone together (Figure 1b).

The slope movement structure in Tepehan, which is the subject of this study, formed during the first major earthquake centred in Pazarcık (Kahramanmaraş), and this has been confirmed by the information received from many local people, some of whom have observed the phenomenon live. In addition, field and UAV-based studies on this structure were completed before the Defne (Hatay) earthquake. Therefore, only the parameters related to the first major earthquake centred in Pazarcık (Kahramanmaraş) will be presented in this section.

Many observatories and seismology centres have provided self-acting (automatic) analysis of this earthquake. They suggested different moment magnitudes and hypocentral locations. For example; AFAD (Republic of Türkiye Ministry of Interior Disaster and Emergency Management Presidency) informed Mw: 7.8 with a hypocentral depth of 18 km, KOERİ (Boğaziçi University, Kandilli Observatory and Earthquake Research Institute Regional Earthquake-Tsunami Monitoring Centre) reported a moment magnitude of 7.7 with a hypocentral depth of 10 km, and finally USGS (United States Geological Survey) solution indicated a Mw: 7.9 earthquake with a hypocentral depth of 33 km (data presented on EMSC; European-Mediterranean Seismological Centre). In seismology-based scientific studies conducted immediately after the earthquake, for example, Melgar et al. (2023) reported its magnitude as Mw: 7.8, relocated the hypocentre at (37.0234° E, 37.2444° N) and the depth as 12 km. On the other hand, the surface rupture has been examined and evaluated by Sümer et al. (2023) using data from field observations, GNSS-RTK module mounted UAV footage, and complementary

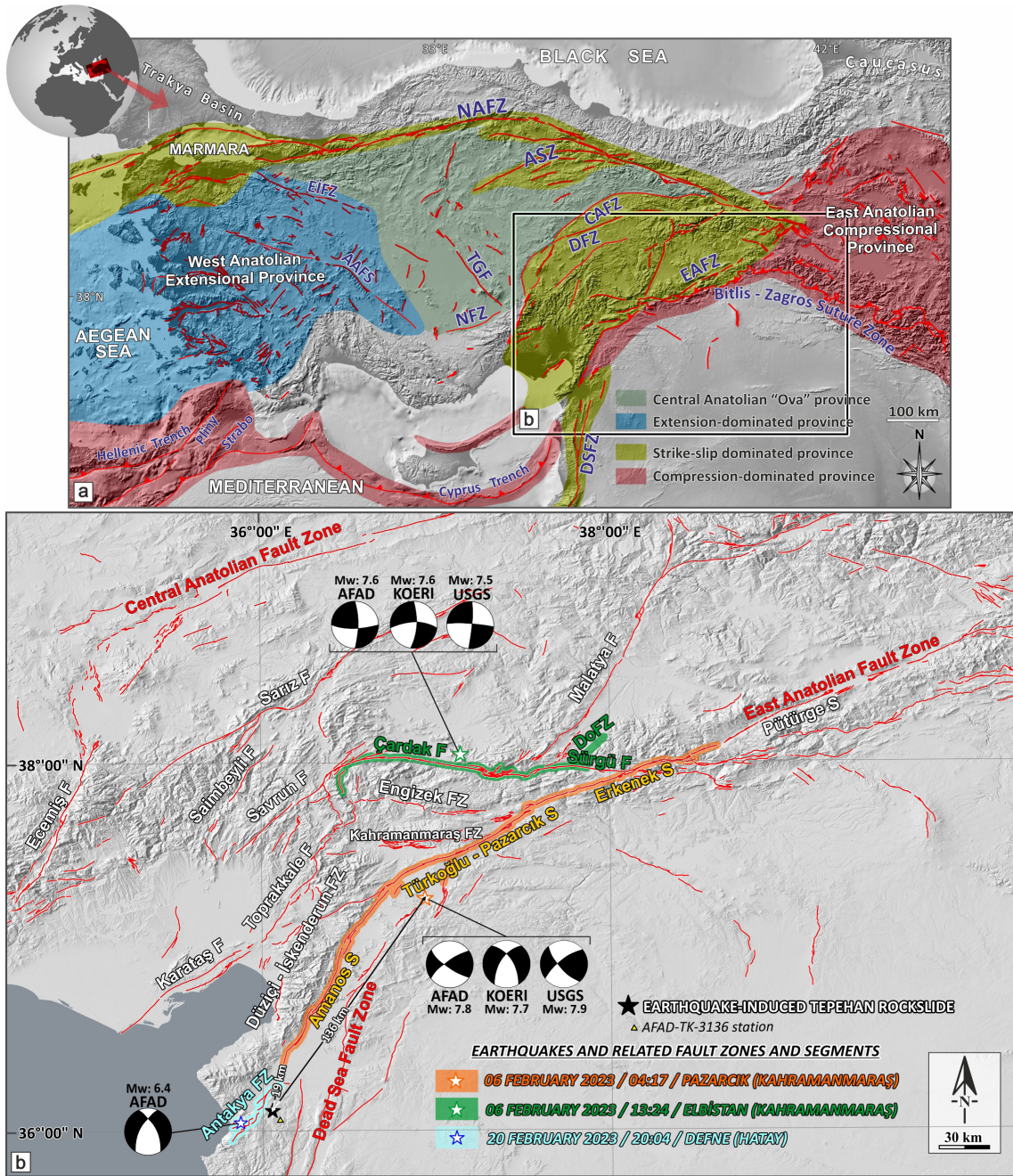


Figure 1. (a) Active tectonic map and structural provinces of Türkiye and surroundings (combined and revised from Şengör et al. 1985; Koçyiğit 2003; Emre et al. 2018; Sümer et al. 2019 and 2023). AAFS: Afyon-Akşehir Fault System, ASZ: Amasya Shear Zone, CAZ: Central Anatolian Fault Zone, DFZ: Deliler Fault Zone, DSFZ: Dead Sea Fault Zone, EAFZ: East Anatolian Fault Zone, EİFZ: Eskişehir-İnönü Fault Zone, NAFZ: North Anatolian Fault Zone, NFZ: Niğde Fault Zone, TGF: Tuz Gölü Faul. (b) Distribution of the main shock epicentres and focal mechanism solutions of the earthquakes, and related tectonic structures affected by the earthquakes. Active faults combined from Karabacak (2007), Karabacak et al. (2012), Meghraoui (2015) and Emre et al. (2018). DoFZ: Doğanşehir Fault Zone. Surface ruptures and impact zones constituted with the information presented in Sümer et al. (2023). Self-acting focal mechanism solution are taken from, AFAD (Republic of Türkiye Ministry of Interior Disaster and Emergency Management Presidency), KOERİ (Boğaziçi University, Kandilli Observatory and Earthquake Research Institute Regional Earthquake-Tsunami Monitoring Centre), and USGS (United States Geological Survey); data presented on EMSC (European-Mediterranean Seismological Centre).

remote sensing methods such as radar interferometry, satellite images, and aerial photographs. They suggested the first major earthquake has formed an approximately 270 km long surface rupture, extending between the south of the Kırıkkhan to the southwest and towards the northeast of Erkenek to the northeast.

4. Material and methods

The standards mentioned in the North American Stratigraphic Commission, 2005 Nomenclature (Easton et al. 2005) rules have been followed for classical stratigraphy studies carried out in the field. In the definition of sedimentary facies, the standards proposed by Miall (1977), Reading (1996), Boggs (2006), and Nichols (2009) were used. Geometry and segmentation terminology for the EAFZ has been adapted from Karabacak et al. (2012), Duman and Emre (2013), and Emre et al. (2018). In this study, Melgar et al. (2023) and Sümer et al.'s (2023) data were used for the seismological parameters of the earthquake and for surface rupture data, respectively. In particular, the relations suggested by Scordilis (2005) were adapted in some earthquake magnitude conversion formulas used in the database collected in this study.

Data were collected in the field with a DJI Phantom 4-Pro Unmanned Aerial Vehicles (UAV), which has a sun correction module, and a Real Time Kinematic (RTK)-Global Navigation Satellite System (GNSS) calibrated from TUSAGA-Aktif (Türkiye National Basic GNSS Network-Active). Three-dimensional and digital elevation models of the slope movement were created by using 562 orthophotos obtained with a resolution of 4.8 cm/px in autonomous flight mode over a total of 24 profiles at an altitude of 100 m (Figures 2a and 2b). All numerical measurements of the structure were performed on these models in centimeter-precision. For the determination of motion vectors and their values, pre-motion images were obtained with Maxar Technology's sub-30 cm/px raster product visualization on Google Earth December 2022 images.

The morphogenetic definition of the slope movement structure, and its formation mechanism in velocity scale, Varnes (1958 and 1978), Cruden and Varnes (1996), Rodríguez et al. (1999), Glastonbury and Fell (2010), Zhou et al. (2016), and Ito et al. (2021) were combined and evaluated. The relations between the earthquake and slope movement parameters have been constructed based on fundamentals proposed by Keefer (1984) and Rodríguez et al. (1999). The details of the archival database especially combined for this study will be given in section six.

5. Field data, modelling, and measurements

This earthquake-induced slope movement structure, which was formed on an olive grove agricultural land, is located in the Altınözü district of Hatay province. The area where

this structure formed is located in a tectonically uplifted corridor controlled by the Antakya Fault Zone (AFZ) to the west and the approximately N-S directed Dead Sea Fault Zone (DFZ) to the east (Figure 1b). Geologically, this structure has formed on the Langhian-Serravalian (Middle Miocene) aged Tepehan formation, which is made up of fine-grained clastic and carbonate rocks and described by Selçuk (1985) and Herece (2008) in detail.

The stratigraphically lower part of the structure is composed of whitish beige-coloured, massive to thick-bedded, well-stratified, well consolidated clayey limestone, marl, and siltstone lithologies, while the upper part is predominantly made of milky-brown coloured thin to thick bedded fine-grained clastic sediments including whitish-coloured carbonate nodules (Figures 3a and 3b). The strike is generally in N-S and NNE-SSW directions and dip angles of the bedding range between 9°E and 11°ESE. The average thickness of the lower consolidated part of the sedimentary package is 9 m, while the thickness of the upper semiconsolidated section is measured 4.5 m. In the lower part, the stratified carbonate and clayey carbonate facies are predominantly in micritic nature and contain green to light grey coloured laminated claystone and mudstone levels that do not exceed 15 cm thickness. Very rare gastropods and ostracods fragments, and sedimentological characteristics of the formation indicate a freshwater lake and lake margin carbonate environment. Almost all sections of the exposed lower stratigraphic part were silicified under the control of the secondary processes after sedimentation, and well compacted parts are characterized by conchoidal fracture with curved breakage surfaces. A soil cover with high caliche content represents the upper levels of the toe section of the structure, and in the easternmost part freshwater small ponds originating from meteoric source leaking between sedimentary packages of the units and/or especially rainfall has been determined (Figures 3c and 3d).

From the measurements on the digitized models, it has been calculated that approximately E-W oriented longest axis of the structure is 496 m, and the widest profile, which extends in the N-S direction is 184 m. Circumference of the structure before the movement is calculated to be 1.23 km, and the area of the total moving mass is estimated to be ca. 71,000 m² (7.1 ha) (Figure 4a). The average thickness of the sliding part of the formation was approximately 13.5 m. The average volume should be at least 1.1 million m³, and with a density of the exposed sedimentary rocks observed in the stratigraphic section, which was assumed to be 2.5 g/cm³, the approximate weight of the total sliding mass should be 2.75 megatons. In addition, the maximum vertical displacement in the disrupted part at the head section of the structure is approximately 3 m, and the vertical distance of the highest fractured section,

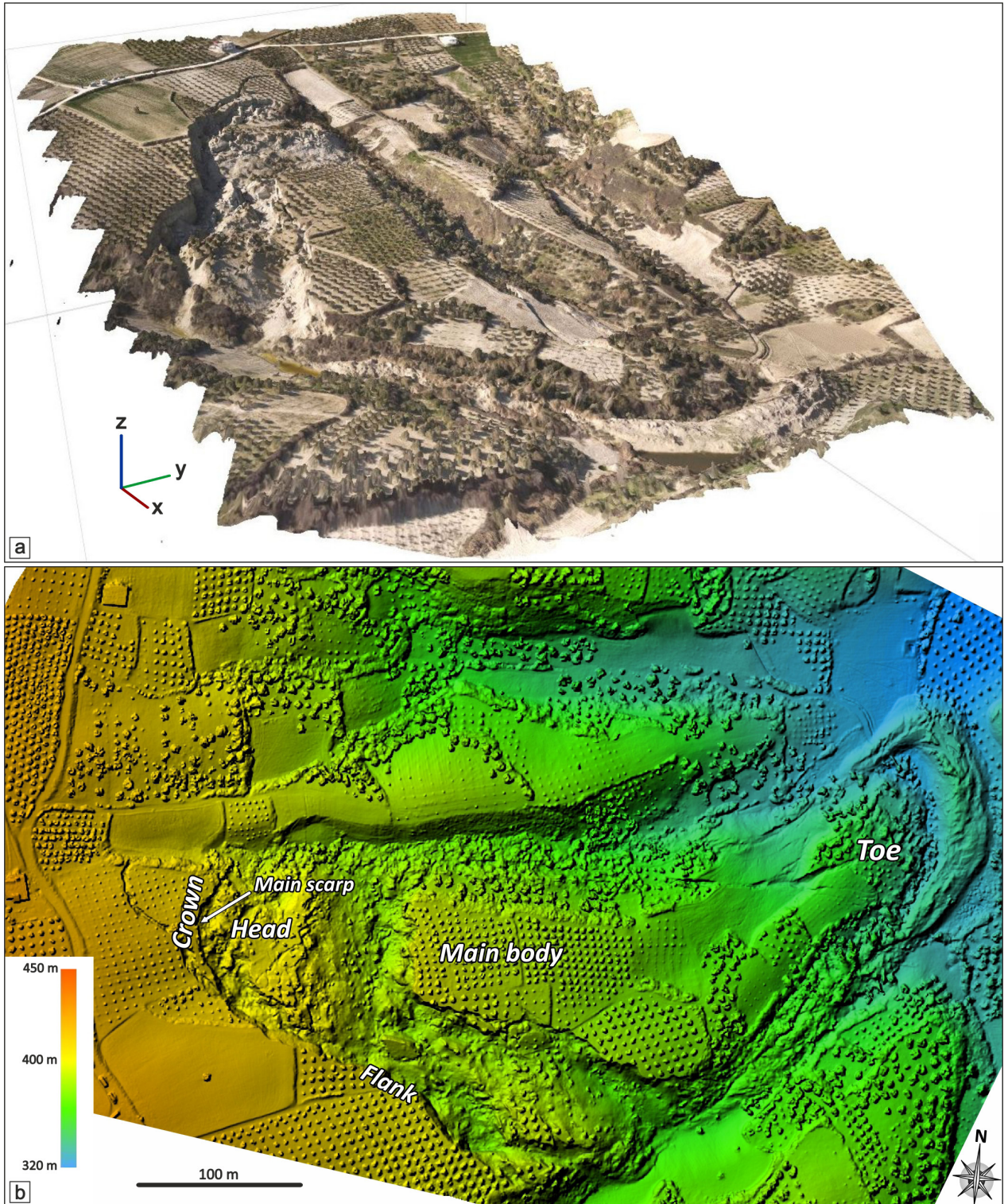


Figure 2. The slope movement in the olive grove in Tepehan village of Hatay province Altınözü district. (a) Three-dimensional (3D) image obtained from orthophotos taken with Unmanned Aerial Vehicles (UAV), (b) Digital elevation model processed with the captured images.

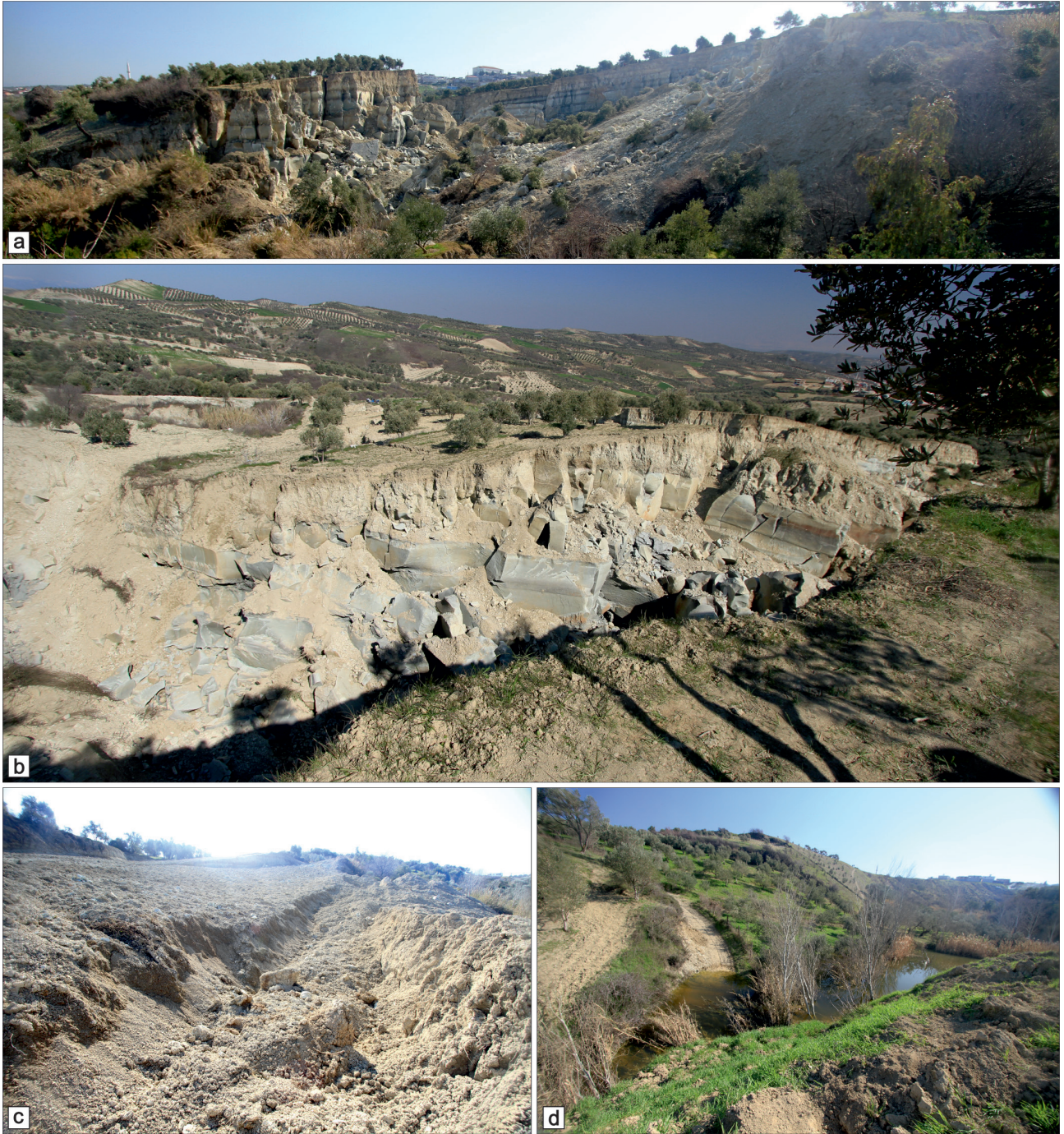


Figure 3. Field photographs of the Tepehan Rockslides (a–b) Panoramic views of exposed outcrops of clayey limestone, marl and fine-grained clastic sedimentary rocks of the Tepehan formation, (c) Whitish-light milky brown coloured soil part with high caliche content forming the upper section of the toe part, (d) freshwater rockslide pond which is formed in front of and juxtaposed to the toe section.

which is located on the southern flank is calculated 16.9 m. A dragged material accumulation in front of the movement with an area of approximately 0.45 ha and 387 m in circumference has reached 9.6 m in height in the toe section of the structure at its eastern termination.

In the inner centre, at the western part of the toe section, the longitudinal offset-cracks reach 8 m horizontally and 2.6 m vertically along the discontinuities lying in approximately E-W direction. These semiparallel cracks are uninterruptedly followed towards the west into the E-W

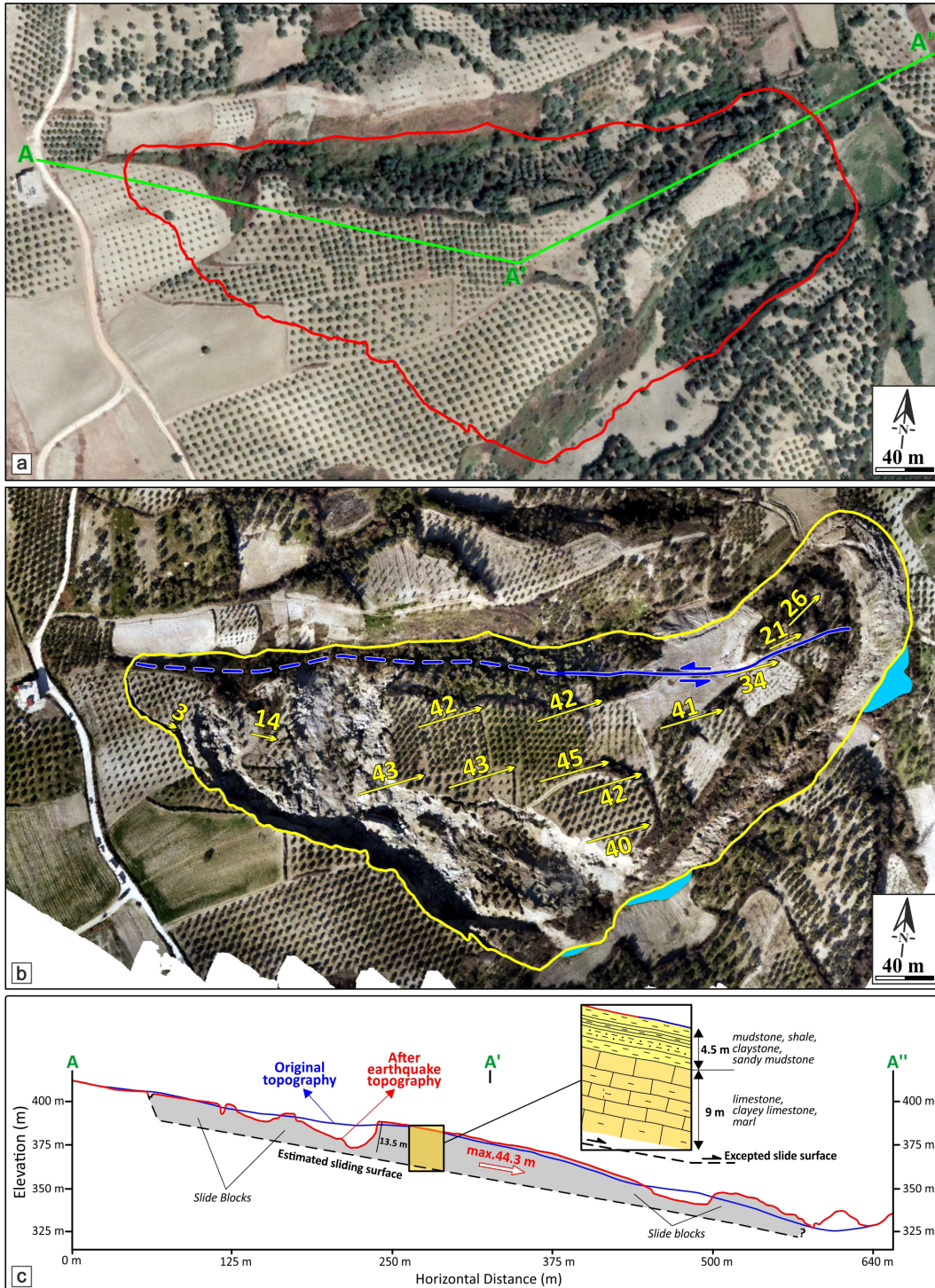


Figure 4. (a and b) Aerial orthophotos before and after the earthquake respectively. The red line shows the main slide body before the movements and the yellow line shows the position after the earthquake. Yellow arrows and numbers show movement directions and amounts on the horizontal plane in meters, green line indicates AA' cross-section, navy blue line represents displaced fracture/crack on the northern edge of the structure and the westward continuation dotted part indicates possible ancient structural discontinuity, blue areas show freshwater ponds. (c) Integrated topographic cross sections on the same ridge (before and after earthquake). Dark blue line shows the original ridge topography by Maxar Technology and the red line indicates after the earthquake by this study.

directed valley, which is located on the northern edge of the structure which is probably characterized by an ancient fault strand. At this point, although the some high-angles planes observed in this valley cuts the Miocene rocks abruptly have been determined, since no clear fault slickenlines and/or kinematic indicators have been determined in these planes, a probabilistic interpretation has been made here.

The images before (Maxar data) and after (UAV data) the earthquake are studied for a morphometric analysis, to determine the mechanism of the movement. The horizontal displacement amounts and directions of 12 locations, those of which the original pre-movement positions were detected before the earthquake, were evaluated (Figure 4b). In addition, an integrated topographic cross section of the subject terrain before and after the earthquake was prepared, in order to determine the morphological change on the ridge (Figure 4c). While the amount of horizontal movement varies between 3 to 14 m in the areas close to the crown part, and 21 to 26 m near the toe section, the greatest displacements are in the range of 40 to 45 m in the middle part of the structure. The motion vectors show that the structure is oriented approximately to the east at its starting point to the west, approximately northeast in the middle part, and north-northeast in the distal part. In the measurements made along approximately E-W trending displaced fracture/crack on the northern edge of the structure, it was determined that the block in the north of the fracture was offset about 10 m less than the southern block, and this situation creates a left lateral offset due to this slightly different motion. All these data show that the movement has started in the western initiation part towards the east and then turned NE direction with a counter-clockwise rotation. The main displacement was accommodated by the structural discontinuity in the northern termination. In comparison of the cross sections little change was observed in the topography of the middle main part of the structure. It was determined that the changes in topography reaching up to 10 m is especially prominent towards the toe part. Three freshwater small ponds with areas of 40, 160, and 315 square m were developed in front of these uplifted sections, along the outermost line running in SW-NE direction, respectively (Figure 4c).

6. Identification of the structure and comparison with similar events on a global-scale

According to the "Classification of Slope Movements" established on the foundations of Varnes (1958 and 1978), the structure that constitutes the main subject of this study is "slide" in terms of movement type, and "translational" due to its sliding surface being a plane. As the sliding material type is a rock and is made of many lithological units, it should be called a "translational rock slide".

In order to make an assessment on the velocity of movement of the structure, firstly the duration of the

subsurface rupture and the earthquake duration felt in the area of the movement should be known. Okuwaki et al. (2023) reported that a sufficiently long maximum slip duration for total source is 80 s. The closest seismic station to the structure is AFAD's TK-3136 Hatay/Altınözü which is located approximately 5.5 km southeast and on the same geological formation with the structure (Figure 1b). For this station, Gülerce et al. (2023) reported, Peak Ground Acceleration (PGA) values of 394 cm/s² in the E-W component and 533 cm/s² in the N-S component, maximum significant duration of 32.73 s, and time interval in the acceleration measurement window to be limited in 110 s. Besides, the information obtained from the local people who were outside during the earthquake is that the formation of structure has terminated during the earthquake and movement was not continued after the earthquake in palpably. Hereby it is expected that the formation time of the structure will probably be completed between 32 to 110 s. The maximum horizontal displacement measured in the middle of the structure is 45 m. When these data are evaluated together, velocity of the movement is calculated to be ranging between 1.4 m/s to 2.4 m/s. These velocity estimates appear to lie between rapid (3m/min) and extremely rapid (5m/s) limits with in the very rapid velocity scale, which was suggested by Cruden and Varnes (1996). From this perspective, in the classification of slope movement velocity scale, the structure should be in the least very rapid class. In another approach; Rodríguez et al. (1999) suggested that earthquake-induced rockslides, according to geometric characteristics, should be divided into two main groups as coherent and disrupted, and disrupted slides in rocks occur preferentially on sedimentary rock material slip surfaces that are predominantly planar in shape. Tepehan translational rockslide has two main bodies separated from each other, especially in its head part meaning it should be classified as disrupted. Movements showing similar morphogenetic characteristics, occurring on low-inclined slide surfaces and having a parallel/semiparallel geological unit bedding with a similar angle-sliding plane were defined as "large rock glide" by Glastonbury and Fell (2010). Since the slope, geological units, and slip plane are close to each other and vary between 9°–11° degrees, Tepehan slope movement can also be considered as a rock glide. In addition, Zhou et al. (2016) classified the earthquake-induced landslides on basis of their volumes. According to their definition small-scaled landslides have volumes less than $10 \times 10^4 \text{ m}^3$, moderate, large-scaled and giant landslides have volumes of $10\text{--}100 \times 10^4 \text{ m}^3$, $100\text{--}500 \times 10^4 \text{ m}^3$, and larger than $500 - 10^4 \text{ m}^3$, respectively. In this perspective, considering at least a $110 - 10^4 \text{ m}^3$ volume of structure moved, the Tepehan translational rockslide should be evaluated as large-scaled. On the other hand, Ito

et al. (2021) also subdivided rockslides into three branches by their topography as “shallow-type”, “slope-type”, and “ridge type”. They also reported that the depth of the slip surface theoretically increases in the order shallow, slope and ridge-types in similar size. According to their classification, if the crown crack or scarp crossed the ridge line with a high angle, and there is a relatively deep sliding surface it can be classified ridge type. There is a very similar geometry in Tepehan rockslide. When all presuggested classifications detailed above are evaluated together, this structure can be defined as “at least very rapid developed translational disrupted ridge-type earthquake-induced large-scaled rockslide or large rock glide”.

In order to compare this earthquake-induced rockslide type slope movement with similar structures on the global-scale, an archival database is compiled in this study from 42 different scientific studies total 34 rockslides (Supplementary material). This archival work shows in general that, the earthquake-induced rockslides can develop medium to large-scale earthquakes ranging between 5.9 to 9.2 moment magnitudes, in all types of geological formations and ages, and they may occur over 200 km away from earthquake epicentre (Figure 5). However, a closer look to this compilation reveals that earthquake-induced rockslides are mostly concentrated in sedimentary rocks and 40 km away from the earthquake epicentres. The parameters required for evaluation on Tepehan Rockslide are; the moment magnitude of the earthquake ($M_w:7.8$), the distance to the epicentre and the surface rupture (136 km and 19 km in respectively), type of the geological formation in which the structure is formed (Middle Miocene aged sedimentary package especially fine-grained clastic and carbonate rocks), and the dimensions of the structure (acreage of moving mass is approximately 7.1 ha and the volume of the structure is at least $110 \times 10^4 \text{ m}^3$). With these specifications, Tepehan Rockslide, is a large-scaled earthquake-induced structure formed farthest from earthquake epicentre distance in the Oligo-Miocene and Pliocene sedimentary rocks. However, the presence of rockslides of much larger size (especially giant scale) which has formed due to even smaller moment magnitude earthquakes and further away from their epicentres suggests that Tepehan Rockslide is not a unique structure. Nevertheless, it is important that, it is the first reported such in detail example known to be classified as earthquake-induced rockslide in Türkiye. In this study, the relations between the earthquake moment magnitude, the distance to the epicentre and surface rupture, and the volume and diversity of the rockslide type slope movement were also evaluated on the compiled database (Figures 6a and 6b). In the basic analyses, best fit on correlation coefficient (R^2) between earthquake moment magnitude to the epicentre and the surface rupture distances are

calculated as 0.56 and 0.54 respectively. These values suggest only a weak to moderate correlation. As can be seen in Figure 6, there are some examples of larger rockslides, formed during smaller earthquake magnitudes, and farther from both the epicentre and the surface rupture. This situation must be related to the inadequacy of the data set and/or the effect of different data inputs (e.g., slope degree, water content, porosity, and other engineering parameters). However, when only the rockslides developed on the Oligo-Miocene and Pliocene sedimentary rocks are evaluated, it is seen that there is a consistency within itself both earthquake magnitude versus distance to epicentre and surface rupture graphics. At this point, it is clear that checking whether this correlation can be strengthened by adding new data to the database is a necessity.

Many other earthquake-induced slope movement structures that developed in the February 2023 earthquakes were also observed during field studies. The most important and well-known of them are as follows: (1) the İdilli landslide, which developed very close to the surface rupture formed during the first major February 6th Pazarcık (Kahramanmaraş) earthquake, has occurred approximately 4 km southwest of İslahiye district of Gaziantep city, reaching 12 ha in areal coverage; (2) a landslide located in the Aşağı İçme neighborhood of Ekinözü district of Kahramanmaraş city that covers more than 15 ha, it was formed adjacent to the surface rupture during the second major earthquake; and (3) small-scaled landslides located around Çökek, Toygarlı, and Karaali neighborhoods of Samandağ and Antakya districts of Hatay city that occurred on February 20th $M_w: 6.4$ Defne (Hatay) earthquake. However, as all the earthquake-induced slope movements were formed by February 2023 earthquakes, Tepehan Rockslide is distinct and largest structure in terms of rockslide type of slope movement.

There are some scientific reasons why such a large structure had been formed that far from the earthquake epicentre. Okuwaki et al. (2023) calculated that the initial earthquake involves a back-propagating supershear rupture, which was started at Pazarcık splay continuing by the initial bifurcated-fault rupture along the main strand of the East Anatolian Fault Zone, and the finally rupture reached to south of the Kırıkhan at its southern termination with a strong directivity of the SW-oriented back rupture process. This strong directivity in the rupture may also tend to increase the local ground acceleration. Actually, the earthquake transferred its last energy towards the south in terms of the rupture mechanism, and the Tepehan Rockslide corresponds to the southward projection of the surface rupture followed to the south of Kırıkhan, which may have also contributed to the formation of the structure. At this point as data reinforcing this interpretation, also at the AFAD station parameters which is very close to the

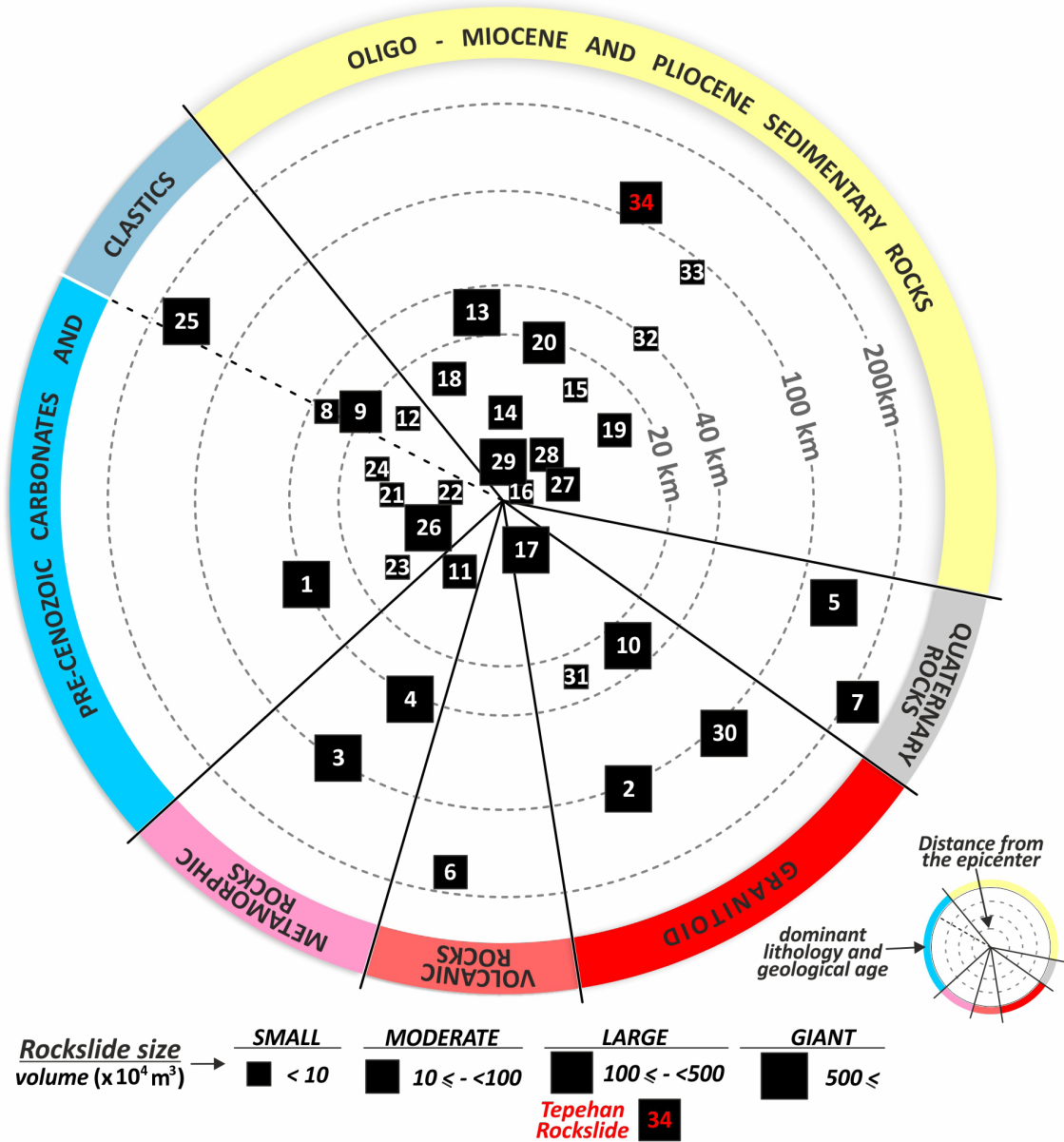


Figure 5. Distributions worldwide earthquake-induced rockslides, their geological units, and distance from epicentre (design of the figure was inspired by Higaki and Abe, 2013). For detail of the descriptions of rockslides please see supplementary material.

structure and located on the same geologic formation, Gülerce et al. (2023) reported PGA values 2 times faster in the N-S component rather than the E-W component. In addition, the lithological features and the internal stratigraphy of the geological formation prone to slope movements and also the presence of probable an ancient fault strand that controls the structure from its northern edge should be an important actor on the formation of the Tepehan Rockslide.

7. Concluding remarks

- Tepehan Rockslide is an at least very rapid developed translational disrupted ridge-type earthquake-induced large-scaled rockslide or large rock glide, which was formed at a distance of 19 km from the surface rupture and 136 km from the epicentre that belongs to the Mw:7.8 February 6th Pazarcık (Kahramanmaraş) earthquake that occurred on the Türkoğlu-Pazarcık, Erkenek, and

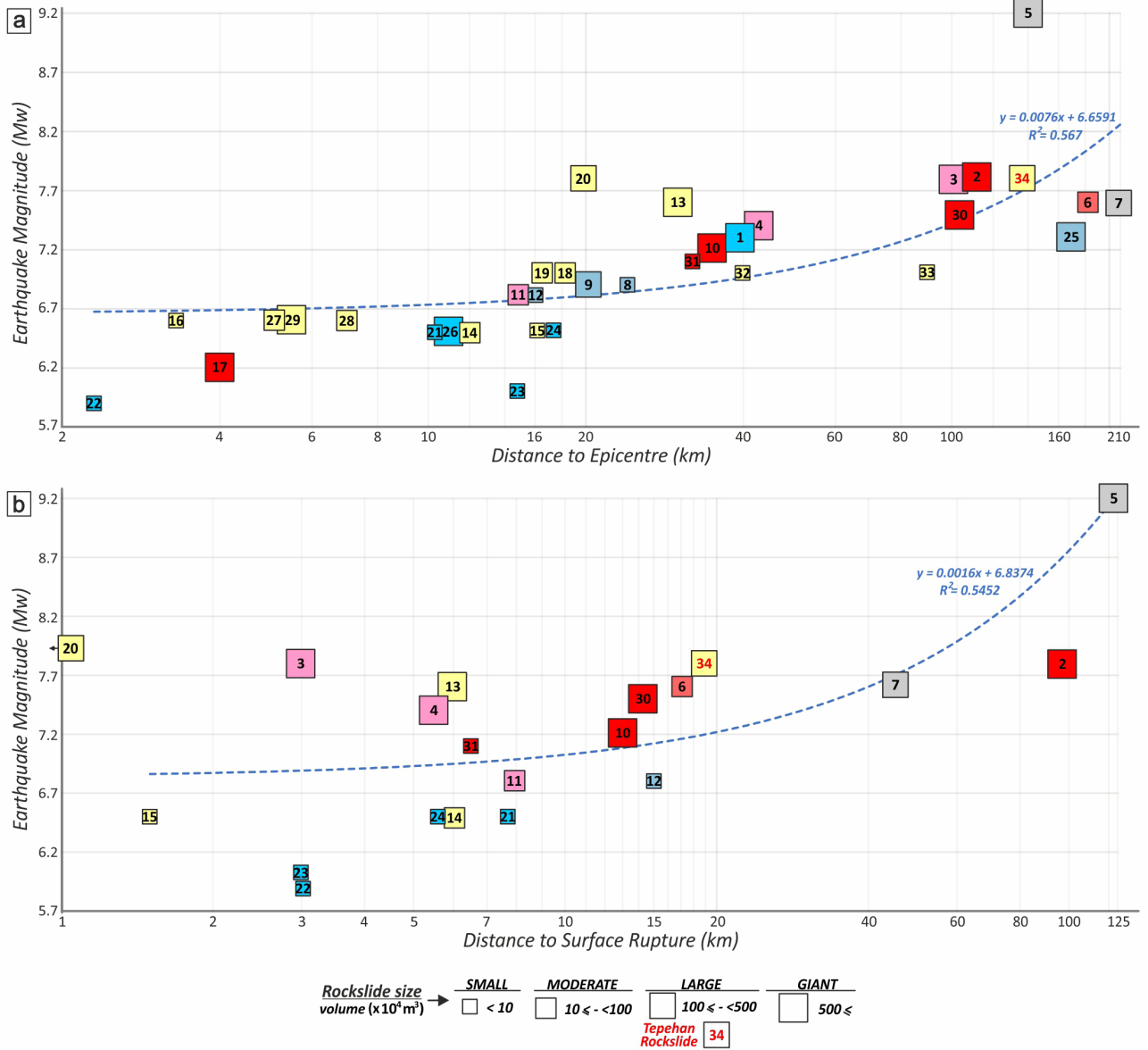


Figure 6. Relations between earthquake moment magnitude and (a) distance to epicentre and distance to (b) surface rupture on earthquake-induced rockslides. For detail of the descriptions of rockslides please see supplementary material. For the colours of the rockslides, please follow the geologic features presented in Figure 5.

Amanos segments of the Eastern Anatolian Fault Zone.

- When the worldwide database compiled is evaluated, it is seen that such an earthquake-induced rockslide so far from the earthquake epicentre is rare, however, it is also noted that such structures have been formed further away from the earthquake epicentre in smaller earthquake magnitudes and in larger volumes. The areal coverage of the slope movements that have occurred in the impact area of the February 2023 earthquakes are large (e.g., Ekinözü/Aşağı İçme

landslide is covering over 15 ha, İdilli landslide is reaching 12 ha). However, although the Tepehan Rockslide covers a smaller surface area of 7.1 ha, it is the largest earthquake-induced slope movement of rockslide type.

- The features of the geological formation in which this structure developed are also noteworthy that it is in an area that corresponds to the projection of the southward extension of the surface rupture observed up to the south of Kırıkhan. On the other hand,

probable an ancient fault structure at the northern boundary of the rockslide seems to control the pattern of the beginning and the continuation of the movement.

- According to Karabacak et al. (2012) there are many paleo landslides, especially along the Erkenek and Türkoğlu segments of the EAFZ and in its immediate part. In addition, the presence of many paleo-slope movement structures in different locations and large areas within the Tepehan formation observed during the field studies indicate that the region has the potential to produce earthquake-induced slope movements in terms of its lithological, topographic, and morphological characteristics. The fact that the region is surrounded by active faults that can produce large earthquake(s) also increases this potential.
- Therefore, this region is an area under the potential risk of the earthquake induced slope movements. It is highly recommended to carry out and produce more scientific studies in terms of geotechnics and engineering geology discipline.

Acknowledgements

I would like to gratefully thank Mahmut Göktuğ Drahor, Semih Eski, Atilla Ongar, Çiğdem Tepe, and especially Ali

Duman for their assistance and help during both field and office work.

I greatly appreciate Ayşegül Askan Gündoğan for scientific discussion and collaboration on ground motion data. I thank Onur Tan for his support of seismological data especially in the magnitude converting process. I am also indebted to Mehmet Akbulut for his critical fundamental contributions. I also thank Tolga Görüm, Mustafa Akyıldız, and Steve Hencher for their valuable contribution to collect the database. Special thanks go to Tell Atchana: Alalakh Excavation Director Murat Akar, excavation worker Berati Sönmez and his family for their accommodation and warm hospitality during the fieldwork. I also thank local people who shared their knowledge and painful experiences with me. Finally, I would like to thank sincerely anonymous referees whose valuable comments and useful criticisms have greatly improved the manuscript. This study was supported by TÜBİTAK National Science Foundation 1002-C Natural Disaster Field Study Emergency Support Program TBK-26. This paper is dedicated to the memory of all people who lost their lives in the earthquakes.

References

- Acar AI (1997) Earthquake-induced landslides. PhD, University of Leeds, Department of Earth Science.
- AFAD, T.C. İçişleri Bakanlığı Afet ve Acil Durum Yönetimi Başkanlığı, <https://deprem.afad.gov.tr/last-earthquakes.html>
- Ambraseys NN (1988). Engineering seismology. *Earthquake Engineering & Structural Dynamics*, 17: 1-105. <https://doi.org/10.1002/eqe.4290170102>
- Arpat E, Şaroğlu F (1972). Doğu Anadolu Fayı ile ilgili bazı gözlemler ve düşünceler. *MTA Dergisi*, 78: 33-39 (in Turkish).
- Arrowsmith JR, Crosby CJ, Korzhenkov AM, Mamyrov E, Povolotskaya I et al. (2017). Surface rupture of the 1911 Kebin (Chon–Kemin) earthquake, Northern Tien Shan, Kyrgyzstan. *Geological Society, London, Special Publications*, 432 (1): 233-253. <https://doi.org/10.1144/sp432.10>
- Aydan Ö, Ulusay R, Atak VO (2008). Evaluation of ground deformations induced by the 1999 Kocaeli earthquake (Turkey) at selected sites on shorelines. *Environmental Geology*, 54: 165-182. <https://doi.org/10.1007/s00254-007-0803-x>
- Baltzer A (1875). Über bergstürze in den Alpen. Verlag der Schabelitz'schen buchhandlung (C. Schmidt) (in German).
- Barka AA (1992). The north Anatolian fault zone. In *Annales tectonicae* (Vol. 6, pp. 164-195).
- Boggs SJR (2006). *Principles of Sedimentology and Stratigraphy*.
- Brandenberg SJ, Idriss IM (2022). An overview of the great Alaska earthquake of 1964.
- Cetin KO, Isik N, Unutmaz B (2004). Seismically induced landslide at Degirmendere Nose, Izmit Bay during Kocaeli (Izmit)-Turkey earthquake. *Soil Dynamics and Earthquake Engineering*, 24 (3): 189-197. <https://doi.org/10.1016/j.soildyn.2003.11.007>
- Cheab A, Lacroix P, Zerathe S, Jongmans D, Ajorlou N et al. (2022). Landslides induced by the 2017 Mw7. 3 Sarpol Zahab earthquake (Iran). *Landslides*, 19 (3): 603-619. <https://doi.org/10.1007/s10346-021-01832-0>
- Chen RF, Chan YC, Angelier J, Hu JC, Huang C et al. (2005). Large earthquake-triggered landslides and mountain belt erosion: the Tsaoiling case, Taiwan. *Comptes Rendus Geoscience*, 337 (13): 1164-1172. <https://doi.org/10.1016/j.crte.2005.04.017>
- Chen TC, Lin ML, Wang KL (2014). Landslide seismic signal recognition and mobility for an earthquake-induced rockslide in Tsaoiling, Taiwan. *Engineering geology*, 171: 31-44. <https://doi.org/10.1016/j.enggeo.2013.11.018>
- Chen K, Xu W, Mai PM, Gao H, Zhang L et al. (2018). The 2017 Mw 7.3 Sarpol Zahab Earthquake, Iran: A compact blind shallow-dipping thrust event in the mountain front fault basement. *Tectonophysics*, 747: 108-114. <https://doi.org/10.1016/j.tecto.2018.09.015>

- Chigira M, Yagi H (2006). Geological and geomorphological characteristics of landslides triggered by the 2004 Mid Niigata prefecture earthquake in Japan. *Engineering Geology*, 82 (4): 202-221. [https://doi.org/10.1016/s0013-7952\(02\)00232-6](https://doi.org/10.1016/s0013-7952(02)00232-6)
- Chigira M, Wang WN, Furuya T, Kamai T (2003). Geological causes and geomorphological precursors of the Tsaoling landslide triggered by the 1999 Chi-Chi earthquake, Taiwan. *Engineering Geology*, 68 (3-4): 259-273.
- Clague JJ, Stead D (editors.). (2012). *Landslides: types, mechanisms and modeling*. Cambridge University Press.
- Cruden DM, Varnes JD (1996). *Landslide types and processes*. Landslides: investigation and mitigation, transportation research board (National Research Council).
- Delvaux D, Abdrakhmatov KE, Lemzin IN, Strom AL (2001). Landslides and surface breaks of the 1911 Ms 8.2 Kemin earthquake, Kyrgyzstan.
- Dewey JE, Şengör AC (1979). Aegean and surrounding regions: complex multiplate and continuum tectonics in a convergent zone. *Geological Society of America Bulletin*, 90 (1): 84-92. [https://doi.org/10.1130/0016-7606\(1979\)90<84:aasrcm>2.0.co;2](https://doi.org/10.1130/0016-7606(1979)90<84:aasrcm>2.0.co;2)
- Duman TY, Çan T, Emre Ö, Keçer M, Doğan A et al. (2005). Landslide inventory of northwestern Anatolia, Turkey. *Engineering geology*, 77 (1-2): 99-114. <https://doi.org/10.1016/j.enggeo.2004.08.005>
- Duman TY, Emre Ö (2013). The East Anatolian Fault: geometry, segmentation and jog characteristics. *Geological Society, London, Special Publications*, 372 (1): 495-529. <https://doi.org/10.1144/sp372.14>
- Easton RM, Jones JO, Lenz AC., Ferrusquía-Villafranca I, Mancini EA et al. (2005). North American commission on stratigraphic nomenclature. *AAPG bulletin*, 89 (11): 1459-1464. <https://doi.org/10.1306/05230505015>
- Emre Ö, Duman TY, Kondo H, Olgun Ş, Özalp S, Elmacı H (2012). 1:250,000 Scale Active Fault Map Series of Turkey, Erzincan (NJ 37-3) Quadrangle. Serial Number: 44, General Directorate of Mineral Research and Exploration, Ankara-Turkey.
- Emre Ö, Duman TY, Özalp S, Şaroğlu F, Olgun Ş et al. (2018). Active fault database of Turkey. *Bulletin of Earthquake Engineering*, 16 (8): 3229-3275. <https://doi.org/10.1007/s10518-016-0041-2>
- EMSC, European-Mediterranean Seismological Centre https://www.emsc-csem.org/Earthquake/index_tensors.php
- Evans SG, Roberts NJ, Ischuk A, Delaney KB, Morozova GS et al. (2009). Landslides triggered by the 1949 Khait earthquake, Tajikistan, and associated loss of life. *Engineering Geology*, 109 (3-4): 195-212. <https://doi.org/10.1016/j.enggeo.2009.08.007>
- Forte G, Verrucci L, Di Giulio A, De Falco M, Tommasi P et al. (2021). Analysis of major rock slides that occurred during the 2016–2017 Central Italy seismic sequence. *Engineering Geology*, 290: 106194. <https://doi.org/10.1016/j.enggeo.2021.106194>
- Glastonbury J, Fell R (2010). Geotechnical characteristics of large rapid rock slides. *Canadian geotechnical journal*, 47 (1): 116-132. <https://doi.org/10.1139/t09-080>
- Görüm T (2016). 23 Ekim 2011 Van depreminin tetiklediği heyelanlar. *Türk Coğrafya Dergisi*, 66: 29-36 (in Turkish). <https://doi.org/10.17211/tcd.69854>
- Gülerce Z, Askan A, Kale Ö, Sandıkkaya A, Işık NS et al. (2023). 6 Şubat 2023 Kahramanmaraş-Pazarcık Mw=7.7 ve Elbistan Mw=7.6 Depremleri Ön Değerlendirme Raporu, Bölüm 4: Kuvvetli Yer Hareketlerinin Ön Analizleri, Orta Doğu Teknik Üniversitesi (in Turkish).
- Hadley J (1960). Landslides and related phenomena accompanying the Hebgen Lake earthquake. *Geological Survey Professional Paper*, 435: 107.
- Hansen WR (1974). Some engineering geologic effects of the 1964 Alaska earthquake. *Annales de la Société géologique de Belgique*.
- Hansen WR, Eckel EB, Schaem WE, Lyle RE, George W et al. (1966). The Alaska earthquake, March 27, 1964: field investigations and reconstruction effort (No. 541). US Geological Survey.
- Harp EL, Wilson RC, Wiczorek GF (1981). Landslides from the February 4, 1976, Guatemala earthquake (No. 551.3 HAR). Washington, DC: US Government Printing Office.
- Harp EL, Jibson RW, Schmitt RG (2016). Map of landslides triggered by the January 12, 2010, Haiti earthquake. US Geological Survey Scientific Investigations Map, 3353, 15.
- Havenith HB (2022). Recent Earthquake-Triggered Landslide Events in Central Asia, Evidence of Seismic Landslides in the Lesser Caucasus and the Carpathians. In *Coseismic Landslides: Phenomena, Long-Term Effects and Mitigation* (pp. 115-141). Singapore: Springer Nature Singapore. https://doi.org/10.1007/978-981-19-6597-5_5
- Havenith HB, Strom A, Jongmans D, Abdrakhmatov A, Delvaux D et al. (2003). Seismic triggering of landslides, Part A: Field evidence from the Northern Tien Shan. *Natural hazards and earth system sciences*, 3 (1/2): 135-149. <https://doi.org/10.5194/nhess-3-135-2003>
- Hencher SR, Acar IA (1995). The Erzincan Earthquake, Friday, 13 March 1992. *Quarterly Journal of Engineering Geology*, 28 (4): 313-316. <https://doi.org/10.1144/gsl.qjegh.1995.028.p4.01>
- Herece E (2008). Atlas of East Anatolian Fault, General Directorate of Mineral Research and Exploration, Special Publication Series-13, 359, 13 appendices as separate maps. ISBN/ISSN: 9786054075126.
- Higaki D, Abe S (2013). Classification of the geomorphology, geology and movement types of earthquake landslides. In *Earthquake-Induced Landslides: Proceedings of the International Symposium on Earthquake-Induced Landslides*, Kiryu, Japan, 2012 (pp. 37-44). Springer Berlin Heidelberg. https://doi.org/10.1007/978-3-642-32238-9_5
- Highland L, Bobrowsky, PT (2008). *The landslide handbook: a guide to understanding landslides* (p. 129). Reston, VA, USA: US Geological Survey.

- Imamura A (1946). A Chain of Landslides as Caused by Seismic Fault. *Proceedings of the Japan Academy*, 22 (8-11): 366-368. <https://doi.org/10.2183/pjab1945.22.366>
- Ito Y, Yamazaki S, Kurahashi T (2021). Geological features of landslides caused by the 2018 Hokkaido Eastern Iwate Earthquake in Japan. *Geological Society, London, Special Publications*, 501 (1): 171-183. <https://doi.org/10.1144/sp501-2019-122>
- Jibson RW (2020). Types and areal distribution of ground failure associated with the 2019 Ridgecrest, California, earthquake sequence. *Bulletin of the Seismological Society of America*, 110 (4): 1567-1578. <https://doi.org/10.1785/0120200001>
- Jibson RW, Prentice CS, Borisoff BA, Rogozhin EA, Langer CJ (1994). Some observations of landslides triggered by the 29 April 1991 Racha earthquake, Republic of Georgia. *Bulletin of the seismological Society of America*, 84 (4): 963-973. <https://doi.org/10.1785/BSSA0840040963>
- Jibson RW, Allstadt KE, Rengers FK, Godt JW (2018). Overview of the geologic effects of the November 14, 2016, Mw 7.8 Kaikoura, New Zealand, earthquake. *Scientific Investigations Report*. <https://doi.org/10.3133/sir20175146>
- Johnson B, Kulikova G, Bergman E, Krueger F, Pierce I et al. (2022, May). Source parameters and locations of the 1949 Mw7. 4 Khait and 1907 Mw7. 6 Karatag earthquakes: implications for how mountain ranges collide. In *EGU General Assembly Conference Abstracts (EGU22-12020)*. <https://doi.org/10.5194/egusphere-egu22-12020>
- Karabacak V (2007). Ölü deniz fay zonu kuzey kesiminin Kuvaterner aktivitesi. PhD, ESOĞÜ, Fen Bilimleri Enstitüsü (in Turkish).
- Karabacak V, Akyüz HS, Kıyak NG, Altunel E, Meghraoui M et al. (2012). Doğu Anadolu Fay Zonu'nun Gölbaşı (Adıyaman) ile Karataş (Adana) arasındaki kesiminin geç Kuvaterner aktivitesi. Tübitak Project, 109Y043 (in Turkish).
- Karakas G, Nefeslioglu HA, Kocaman S, Buyukdemircioglu M, Yurur T et al. (2021). Derivation of earthquake-induced landslide distribution using aerial photogrammetry: the January 24, 2020, Elazığ (Turkey) earthquake. *Landslides*, 18 (6): 2193-2209. <https://doi.org/10.1007/s10346-021-01660-2>
- Keefer DK (1984). Landslides caused by earthquakes. *Geological Society of America Bulletin*, 95 (4): 406-421. [https://doi.org/10.1130/0016-7606\(1984\)95<406:lcb>2.0.co;2](https://doi.org/10.1130/0016-7606(1984)95<406:lcb>2.0.co;2)
- Keefer DK (2002). Investigating landslides caused by earthquakes—a historical review. *Surveys in geophysics*, 23: 473-510. <https://doi.org/10.1023/A:1021274710840>
- Koçyiğit A (2003). General neotectonic characteristics and seismicity of Central Anatolia. TPJD, special publication, 5: 1-26.
- KOERI, Boğaziçi Üniversitesi Kandilli Rasathanesi ve Deprem Araştırma Enstitüsü (KRDAE) Bölgesel Deprem-Tsunami İzleme ve Değerlendirme Merkezi (BDTİM): <http://www.koeri.boun.edu.tr/scripts/1st6.asp>
- Köküm M (2021). Landslides and lateral spreading triggered by the 24 January 2020 Sivrice earthquake (East Anatolian Fault). *Gümüşhane Üniversitesi Fen Bilimleri Dergisi*, 11 (3): 751-760. <https://doi.org/10.17714/gumusfenbil.877544>
- Kulikova G, Schurr B, Krüger F, Brzoska E, Heimann S (2016). Source parameters of the Sarez-Pamir earthquake of 1911 February 18. *Geophysical Journal International*, 205 (2): 1086-1098. <https://doi.org/10.1093/gji/ggw069>
- Kuşçu İ, Okamura M, Matsuoka H, Gökaşan E, Awata Y et al. (2005). Seafloor gas seeps and sediment failures triggered by the August 17, 1999 earthquake in the Eastern part of the Gulf of İzmit, Sea of Marmara, NW Turkey. *Marine Geology*, 215 (3-4): 193-214. <https://doi.org/10.1016/j.margeo.2004.12.002>
- Ling S, Sun C, Li X, Ren Y, Xu J et al. (2021). Characterizing the distribution pattern and geologic and geomorphic controls on earthquake-triggered landslide occurrence during the 2017 Mw 7.0 Jiuzhaigou earthquake, Sichuan, China. *Landslides*, 18: 1275-1291. <https://doi.org/10.1007/s10346-020-01549-6>
- Lovelock PER (1984). A review of the tectonics of the northern Middle East region. *Geological Magazine*, 121 (6): 577-587. <https://doi.org/10.1017/s0016756800030727>
- Mahdavi MR, Solaymani S, Jafari MK (2006). Landslides triggered by the Avaj, Iran earthquake of June 22, 2002. *Engineering geology*, 86 (2-3): 166-182. <https://doi.org/10.1016/j.enggeo.2006.02.016>
- Massey C, Townsend D, Rathje E, Allstadt KE, Lukovic B et al. (2018). Landslides Triggered by the 14 November 2016 Mw 7.8 Kaikōura Earthquake, New Zealand. *Bulletin of the Seismological Society of America*, 108 (3B): 1630-1648. <https://doi.org/10.1785/0120170305>
- Maxar Technologies, <https://www.maxar.com/>
- McKenzie D (1976). The East Anatolian Fault: a major structure in eastern Turkey. *Earth and Planetary Science Letters*, 29 (1): 189-193. [https://doi.org/10.1016/0012-821x\(76\)90038-8](https://doi.org/10.1016/0012-821x(76)90038-8)
- Meghraoui M (2015). Paleoseismic History of the Dead Sea Fault Zone. *Encyclopedia of Earthquake Engineering*. DOI 10.1007/978-3-642-36197-5_40-1.
- Melgar D, Taymaz T, Ganas A, Crowell BW, Öcalan T et al. (2023). Sub- and super-shear ruptures during the 2023 Mw 7.8 and Mw 7.6 earthquake doublet in SE Türkiye. *SEISMICA*, 2 (3): 1-10. <https://doi.org/10.31223/x52w9d>
- Miall AD (1977). A review of the braided-river depositional environment. *Earth-Science Reviews*, 13 (1): 1-62. [https://doi.org/10.1016/0012-8252\(77\)90055-1](https://doi.org/10.1016/0012-8252(77)90055-1)
- Muehlberger WR, Gordon MB (1987). Observations on the complexity of the East Anatolian Fault, Turkey. *Journal of Structural Geology*, 9 (7): 899-903. [https://doi.org/10.1016/0191-8141\(87\)90091-5](https://doi.org/10.1016/0191-8141(87)90091-5)
- NLA, National Library of Australia <https://nla.gov.au/nla.obj-232871964/view?showBrowseWidget=true&showBrowseView=index>
- Nichols G (2009). *Sedimentology and stratigraphy*. John Wiley & Sons.
- Ocakoglu F, Tuncay E (2023). Geological and geomechanical evidence from the Sünnet landslides (NW Anatolia) for an Mw8. 0 cascade rupture in the North Anatolian Fault 8 ky ago. *Tectonophysics*, 846: 229682. <https://doi.org/10.1016/j.tecto.2022.229682>

- Okuwaki R, Yuji Y, Taymaz T, Hicks SP (2023). Multi-scale rupture growth with alternating directions in a complex fault network during the 2023 south-eastern Türkiye and Syria earthquake doublet. *Geophysical Research Letters*, 50 (12): e2023GL103480. <https://doi.org/10.31223/x5rd4w>
- Oppikofer T, Hermanns RL, Redfield TF, Sepúlveda SA, Duhart P et al. (2012). Morphologic description of the Punta Cola rock avalanche and associated minor rockslides caused by the 21 April 2007 Aysén earthquake (Patagonia, southern Chile). *Revista de la Asociación Geológica Argentina*, 69 (3): 339-353.
- Oswald F (1906). *A Treatise on the Geology of Armenia*. PhD, University of London.
- Papadopoulos GA, Plessa A (2000). Magnitude–distance relations for earthquake-induced landslides in Greece. *Engineering Geology*, 58 (3-4): 377-386. [https://doi.org/10.1016/s0013-7952\(00\)00043-0](https://doi.org/10.1016/s0013-7952(00)00043-0)
- Perez JS, Llamas DCE, Dizon MP, Buhay DJL, Legaspi CJM et al. (2023). Impacts and causative fault of the 2022 magnitude (Mw) 7.0 Northwestern Luzon earthquake, Philippines. *Frontiers in Earth Science*, 11: 1091595. <https://doi.org/10.3389/feart.2023.1091595>
- Perinçek D, Çemen I (1990). The structural relationship between the East Anatolian and Dead Sea fault zones in southeastern Turkey. *Tectonophysics*, 172 (3-4): 331-340. [https://doi.org/10.1016/0040-1951\(90\)90039-b](https://doi.org/10.1016/0040-1951(90)90039-b)
- Pınar N, Lahn E (1952). *Türkiye Depremleri İzahlı Kataloğu 6-36*. T.C. Bayındırlık Bakanlığı Yapı ve İmar İşleri Yayınları, Ankara (in Turkish).
- Plafker G (1969). *Tectonics of the March 27, 1964, Alaska earthquake*. U.S. Geological Survey Professional Paper 543–I. <https://doi.org/10.3133/pp543i>
- Ponti DJ, Blair JL, Rosa CM, Thomas K, Pickering AJ et al. (2020). Documentation of surface fault rupture and ground-deformation features produced by the 4 and 5 July 2019 Mw 6.4 and Mw 7.1 Ridgecrest earthquake sequence. *Seismological Research Letters*, 91 (5): 2942-2959. <https://doi.org/10.1785/0220190322>
- Porfido S, Esposito E, Spiga E, Sacchi M, Molisso F et al. (2015). Impact of ground effects for an appropriate mitigation strategy in seismic area: the example of Guatemala 1976 earthquake. In *Engineering Geology for Society and Territory-Volume 2: Landslide Processes* (pp. 703-708). Cham: Springer International Publishing. https://doi.org/10.1007/978-3-319-09057-3_117
- Reading HG (editor) (1996). *Sedimentary environments: processes, facies and stratigraphy*. Third edition, John Wiley & Sons.
- Redfield T, Hermanns R, Oppikofer T, Duhart P, Mella M et al. (2011). Analysis of the 2007 earthquake-induced Punta Cola rockslide and tsunami, Aysén fjord, Patagonia, Chile (45.3 ° s, 73.0 w). In *5th international conference on earthquake geotechnical engineering*, Santiago, paper (Vol. 12).
- Rimando J, Williamson A, Mendoza RB, Hobbs T (2022). Source Model and Characteristics of the 27 July 2022 MW 7.0 Northwestern Luzon Earthquake, Philippines. *Seismica*, 1 (1). <https://doi.org/10.26443/seismica.v1i1.217>
- Rodríguez CE, Bommer JJ, Chandler RJ (1999). Earthquake-induced landslides: 1980–1997. *Soil Dynamics and Earthquake Engineering*, 18 (5): 325-346. [https://doi.org/10.1016/s0267-7261\(99\)00012-3](https://doi.org/10.1016/s0267-7261(99)00012-3)
- Schuster RL, Alford D (2004). Usoi Landslide Dam and Lake Sarez, Pamir Mountains, Tajikistan. *Environmental and Engineering Geoscience*, 10 (2): 151-168. <https://doi.org/10.2113/10.2.151>
- Scordilis EM (2005, September). Globally valid relations converting Ms, mb and MJMA to Mw. In *Meeting on earthquake monitoring and seismic hazard mitigation in Balkan Countries*, NATO ARW, Borovetz, Bulgaria (pp. 11-17).
- Seed HB (1968). The fourth Terzaghi lecture: Landslides during earthquakes due to liquefaction. *Journal of the Soil Mechanics and Foundations division*, 94 (5): 1053-1122. <https://doi.org/10.1061/jfsfaq.0001182>
- Selçuk H (1985). Kızıldağ-Keldağ-Hatay dolayının jeolojisi ve jeodinamik evrimi. MTA Raporu, (7787) (in Turkish).
- Şengör AMC, Görür N, Şaroğlu F (1985). Strike-slip faulting and related basin formation in zones of tectonic escape: Turkey as a case study. In: Biddle KT, Christie-Blick N (editors). *Strike-Slip deformation, basin formation, and sedimentation*. Tulsa, OK: Society of Economic Paleontologists and Mineralogists, 37, pp. 227-264.
- Shao X, Ma S, Xu C (2023). Distribution and characteristics of shallow landslides triggered by the 2018 Mw 7.5 Palu earthquake, Indonesia. *Landslides*, 20 (1): 157-175. <https://doi.org/10.1007/s10346-022-01972-x>
- Sieberg A (1932). *Erdbeben geographie: Handbuch der Geophysik, v. IV: Berlin* (in German).
- Smith GI (2009). Late Cenozoic geology and lacustrine history of Searles Valley, Inyo and San Bernardino Counties, California (p. 115). US Geological Survey. Professional Paper 172. <https://doi.org/10.3133/pp1727>
- Sümer Ö, Drahor MG, Berge MA, Ongar A, Schachner A (2019). Geoarchaeological and archaeoseismological observations in Hattuşa: first evidence of earthquake traces from the Hittite Capital. *Archäologischer Anzeiger*, 1: 90-96.
- Sümer Ö, Drahor MG, Ongar A, Eski S, Tepe Ç et al. (2023). 06 Şubat 2023 04:17, Mw=7.7 Pazarcık (Kahramanmaraş): 06 Şubat 2023 13:24, Mw=7.6 Elbistan (Kahramanmaraş) ve 20 Şubat 2023 20:04, Mw=6.4 Defne (Hatay) Depremleri, Saha Çalışmaları Yerbilimsel Ön Raporu 1, Dokuz Eylül Üniversitesi (in Turkish).
- Tanyaş H, Van Westen CJ, Allstadt KE, Anna Nowicki Jessee M, Görüm T et al. (2017). Presentation and analysis of a worldwide database of earthquake-induced landslide inventories. *Journal of Geophysical Research: Earth Surface*, 122 (10): 1991-2015. <https://doi.org/10.1002/2017jf004236>

- Tatar O, Piper JDA, Gürsoy H, Heimann A, Koçbulut F (2004). Neotectonic deformation in the transition zone between the Dead Sea Transform and the East Anatolian Fault Zone, Southern Turkey: a palaeomagnetic study of the Karasu Rift Volcanism. *Tectonophysics*, 385 (1-4): 17-43. <https://doi.org/10.1016/j.tecto.2004.04.005>
- Türkiye Ulusal Sabit GNSS Ağı – Aktif, <https://www.tusaga-aktif.gov.tr/>
- USGS, United States Geological Survey, <https://www.usgs.gov/>
- Vakarchuk RN, Tatevossian RE, Aptekman ZY, Bykova VV (2013). The 1991 Racha earthquake, Caucasus: Multiple source model with compensative type of motion. *Izvestiya, Physics of the Solid Earth*, 49: 653-659. <https://doi.org/10.1134/s1069351313050121>
- Varnes DJ (1958). Landslide types and processes. In: Eckel EB (editor). *Landslides and Engineering Practice*. Washington: NAS-NRC Publication 544: pp. 20-47.
- Varnes DJ (1978). Slope movement types and processes. *Special report*, 176: 11-33.
- Xu C, Shyu JBH, Xu X (2014). Landslides triggered by the 12 January 2010 Port-au-Prince, Haiti, M_W= 7.0 earthquake: visual interpretation, inventory compiling, and spatial distribution statistical analysis. *Natural Hazards and Earth System Sciences*, 14 (7): 1789-1818. <https://doi.org/10.5194/nhess-14-1789-2014>
- Yamada M, Wang G, Mukai K (2013). The classification and features of earthquake-induced landslides in the world. In *Earthquake-Induced Landslides: Proceedings of the International Symposium on Earthquake-Induced Landslides*, Kiryu, Japan, 2012 (pp. 117-124). Springer Berlin Heidelberg. https://doi.org/10.1007/978-3-642-32238-9_13
- Yönlü, Ö., Altunel, E., & Karabacak, V. (2017). Geological and geomorphological evidence for the southwestern extension of the East Anatolian Fault Zone, Turkey. *Earth and Planetary Science Letters*, 469: 1-14. <https://doi.org/10.1016/j.epsl.2017.03.034>
- Zhou JW, Lu PY, Hao MH (2016). Landslides triggered by the 3 August 2014 Ludian earthquake in China: geological properties, geomorphologic characteristics and spatial distribution analysis. *Geomatics, Natural Hazards and Risk*, 7 (4): 1219-1241. <https://doi.org/10.1080/19475705.2015.1075162>

Supplementary material

Number	Year	Earthquake	Earthquake Type	Magnitude	Magnitude (Mw)	Focal Depth (km)	Geological Age and Lithology	Lithology Code	* Distance to Epicenter (km)	* Distance to Rupture (km)	Rockslide Type	Area (x10 ³) (m ²)	Volume (x10 ⁷) (m ³)	References Code	References
1	1911	Sarez, TAJIKISTAN	Sinistral	7.3 (Mw)	7.3	26	Pre-Cenozoic Carbonates and Clastics (Permio-Triassic Carbonate Rocks)	6	39.4	No Rupture	Massive Rockslide	4000*	200000	a	Haventh (2022)
2	1911	Kemln, KYRGYZSTAN	Reverse	7.8 (Mw)	7.8	20	Granitoid (Palaeozoic Granite)	4	109.0	97	Rockslide	150	3000	b	Kulhova et al. (2016)
3	1911	Kemln, KYRGYZSTAN	Reverse	7.8 (Mw)	7.8	20	Metamorphic Rocks (Proterozoic basic sedimentary)	7	101.0	3	Rockslide	116.2*	500	c	Schuster and Alford (2004)
4	1949	Khat, TAJIKISTAN	Reverse	7.4 (Mw)	7.4	18	Pre-Cenozoic Carbonates and Clastics (Pre-Tertiary Gneiss Schist)	7	42.2	5.5	Rockslide	300*	7500	d	Aronsmith et al. (2017)
5	1964	Alaska, USA	Reverse	9.2 (Mw)	9.2	20	Quaternary Rocks (Pleistocene Glaciolacustrine Deposit)	1	140.0	123	Translational Landslide	40*	2400	e	Haventh et al. (2003)
6	1976	Los Amates, GUATEMALA	Sinistral	7.6 (Mw)	7.6	5	Volcanic Rocks (Cenozoic volcanics)	3	182.1	171*	Blockslide	10*	200	f	Delvaux et al. (2001)
7	1976	Los Amates, GUATEMALA	Sinistral	7.6 (Mw)	7.6	5	Quaternary Rocks (Pleistocene Volcaniclastic Rocks)	1	209.7	45.2	Blockslide	17*	100	g	Johnson et al. (2022)
8	1991	Racha, GEORGIA	Reverse	6.9 (Mw)	6.9	17	Pre-Cenozoic Carbonates and Clastics (Cretaceous Limestone-Shale)	5	24.0	No Rupture	Rock-block slide	0.013*	2	o,p	Evens et al. (2009)
9	1991	Racha, GEORGIA	Reverse	6.9 (Mw)	6.9	17	Pre-Cenozoic Carbonates and Clastics (Cretaceous Limestone-Shale)	5	20.2	No Rupture	Rock-block slide	13*	200	o,p	Hansen et al. (1986)
10	1992	Suusamyr, KYRGYZSTAN	Reverse	7.2 (Mw)	7.2	17	Granitoid (Palaeozoic Granite)	4	35.0	13	Rockslide	82*	2000	a	Brandenberg and Gfriss (2022)
11	1992	Ertisay, TÜRKİYE	Dextral	6.8 (Mw)	6.8	28	Metamorphic Rocks (Palaeozoic schist)	7	15.0	8	Rock-block slide	?	50	an,ao	Pfahler (1969)
12	1992	Ertisay, TÜRKİYE	Dextral	6.8 (Mw)	6.8	28	Pre-Cenozoic Carbonates and Clastics (Mesozoic Shale)	5	16.0	15	Planar rock block slide	0.36	1.4	an,ao	Hansen (1974)
13	1999	Chi-Chi, TAIWAN	Reverse	7.6 (Mw)	7.6	10	Oligo-Miocene and Pliocene Sedimentary Rocks (Pliocene Sedimentary Rocks)	2	30.0	6	Rockslide	1600	12500	q,r,s	Harp et al. (1981)
14	2002	Avaj, IRAN	Reverse	6.5 (Mw)	6.5	10	Oligo-Miocene and Pliocene Sedimentary Rocks (Oligo-Miocene Sedimentary Rocks)	2	11.5	6	Rockslide	1.1*	11	t	Porfido et al. (2015)
15	2002	Avaj, IRAN	Reverse	6.5 (Mw)	6.5	10	Oligo-Miocene and Pliocene Sedimentary Rocks (Oligo-Miocene Sedimentary Rocks)	2	16.7	1.5	Rock-block slide	0.075*	0.15	t	Jibson et al. (1994)
16	2004	Mid-Niiga, JAPAN	Reverse	6.6 (Mw)	6.6	15	Oligo-Miocene and Pliocene Sedimentary Rocks (Pliocene Sedimentary Rocks)	2	3.3	No Rupture	Rockslide	1.6	2.3	u	Vakarchuk et al. (2013)
17	2007	Punta Gsa, CHILE	Sinistral	6.2 (Mw)	6.2	12	Granitoid (Neogene Granitic Rock)	4	4.0	No Rupture	Rockslide	43*	2440	v,w	Chen et al. (2006)
18	2010	Port au Prince, HAITI	Sinistral	7.0 (Mw)	7.0	13	Oligo-Miocene and Pliocene Sedimentary Rocks (Miocene Sedimentary Rocks)	2	17.8	No Rupture	Rockslide	4.4	20	x,y	Chigira et al. (2003)
19	2010	Port au Prince, HAITI	Sinistral	7.0 (Mw)	7.0	13	Oligo-Miocene and Pliocene Sedimentary Rocks (Miocene Sedimentary Rocks)	2	16.8	No Rupture	Rockslide	2.4	10	x,y	Chen et al. (2014)
20	2016	Kaikoura, NEW ZEALAND	Reverse	7.8 (Mw)	7.8	15	Oligo-Miocene and Pliocene Sedimentary Rocks (Neogene Siltstone)	2	19.8	0	Translational Rockslide	20	200	z,aa	MahdaviFar et al. (2006)
21	2016	Norcia, ITALY	Normal	6.5 (Mw)	6.5	9	Pre-Cenozoic Carbonates and Clastics (Early Cretaceous Carbonate Rocks)	6	10.3	7.7	Rockslide	1.7*	3.2	ab	Chigira and Yagi (2006)
22	2016	Visso, ITALY	Normal	5.9 (Mw)	5.9	8	Pre-Cenozoic Carbonates and Clastics (Early Cretaceous Carbonate Rocks)	6	2.3	3	Rockslide	0.02*	0.04	ab	Redfield et al. (2011)
23	2016	Amarfice, ITALY	Normal	6.0 (Mw)	6.0	8	Pre-Cenozoic Carbonates and Clastics (Early Jurassic Carbonate Rocks)	6	14.9	3	Rockslide	0.098	1.5	ab	Oppolzer et al. (2012)
24	2016	Norcia, ITALY	Normal	6.5 (Mw)	6.5	9	Pre-Cenozoic Carbonates and Clastics (Early Cretaceous Carbonate Rocks)	6	16.8	5.6	Rockslide	0.48	1.5	ab	Xu et al. (2014)
25	2017	Sarpei Zahab, IRAN	Reverse	7.3 (Mw)	7.3	15	Pre-Cenozoic Carbonates and Clastics (Mesozoic Shale)	5	169.7	No Rupture	Giant Rockslide	5800	52000	ac,ad	Harp et al. (2016)
26	2017	Juzhaiguo, CHINA	Sinistral	6.5 (Mw)	6.5	20	Pre-Cenozoic Carbonates and Clastics (Middle Carboniferous Carbonate Rocks)	6	10.9	No Rupture	Rockslide	30*	570*	ae	Jibson et al. (2018)
27	2018	Iburi, JAPAN	Reverse	6.6 (Mw)	6.6	37	Oligo-Miocene and Pliocene Sedimentary Rocks (Miocene Sedimentary Rocks)	2	5.2	No Rupture	Ridge-type Rockslide	2.1*	21*	af	Massev et al. (2018)
28	2018	Iburi, JAPAN	Reverse	6.6 (Mw)	6.6	37	Oligo-Miocene and Pliocene Sedimentary Rocks (Miocene Sedimentary Rocks)	2	7.0	No Rupture	Ridge-type Rockslide	1.4*	14*	af	Forté et al. (2021)
29	2018	Iburi, JAPAN	Reverse	6.6 (Mw)	6.6	37	Oligo-Miocene and Pliocene Sedimentary Rocks (Miocene Sedimentary Rocks)	2	5.1	No Rupture	Ridge-type Large Rockslide	30	5400*	af	Chen et al. (2018)
30	2018	Palu, INDONESIA	Sinistral	7.5 (Mw)	7.5	10	Granitoid (Mid-Pliocene Granite-Diorite)	4	104.0	14.3	Rockslide	95.2*	2070*	ag	Chehb et al. (2022)
31	2019	Ridgecrest, USA	Dextral	7.1 (Mw)	7.1	8	Granitoid (Mesozoic Granite)	4	32.0	6.5	Rockslide	0.025*	0.05*	ah,ai,aj	Lung et al. (2021)
32	2022	Luzon, PHILIPPINES	Reverse	7.0 (Mw)	7.0	15	Oligo-Miocene and Pliocene Sedimentary Rocks (Oligo-Miocene Sedimentary Rocks)	2	40.0	No Rupture	Translational Slide - Rockslide	3*	6*	ak,al,am	Ito et al. (2021)
33	2022	Luzon, PHILIPPINES	Reverse	7.0 (Mw)	7.0	15	Oligo-Miocene and Pliocene Sedimentary Rocks (Oligo-Miocene Sedimentary Rocks)	2	90.0	No Rupture	Massive Rockslide	0.47*	8.54*	ak,al,am	Shao et al. (2023)
34	2023	Kahramanmaraş, TÜRKİYE	Sinistral	7.8 (Mw)	7.8	12	Oligo-Miocene and Pliocene Sedimentary Rocks (Pliocene Sedimentary Rocks)	2	136.0	19	Rockslide	7.1	110	This Study	Smith (2009)

converted by Scordilis (2005) Mjma and Ms / * calculated in this study with data obtained from the cited references